JOURNAL OF COMPUTATIONAL PHYSICS 114, 176–184 (1994)

Ellipticity, Accuracy, and Convergence of the Discrete Navier–Stokes Equations

S. W. ARMFIELD

Department of Civil and Environmental Engineering, University of Western Australia, Perth, Western Australia 6009

Received December 16, 1992; revised August 1, 1993

The introduction into the continuity equation of additional terms to recover grid-scale ellipticity, for the Navier–Stokes equations discretised on a non-staggered mesh, results in an increase in the discretisation error. The introduced error is a combination of the additional truncation error and a false source resulting from the inconsistent construction of the conservation equations used in the finite volume scheme considered. The false source error component is removed by constructing the conservation terms consistently, while the additional truncation error is shown to be of the same order as the leading order truncation error associated with the unmodified equations. A method of reducing the magnitude of the additional terms, thereby reducing the additional error, is considered. It is shown that although this does reduce the magnitude of the error it also reduces the ellipticity of the equations and leads to slower convergence.

1. INTRODUCTION

When the Navier–Stokes equations are discretized on a non-staggered mesh, with all the unknowns stored at the same locations and second-order central differencing used for the pressure gradient and continuity terms, a grid scale oscillation is seen to develop in the pressure field. This behaviour is the result of the discrete system being non-elliptic at the grid scale wave number. Several methods have been suggested to recover the full ellipticity of the discrete system and prevent the occurrence of this oscillation [1–5]. In Armfield [1] a finite volume method was presented that was specifically designed to have an identical discrete ellipticity to the finite volume SIMPLE scheme defined on a staggered mesh [6–9], which in turn has an identical discrete ellipticity to the standard second-order central differencing for the Laplace operator. The Armfield scheme, which is briefly described in the next section, was obtained by adding additional terms into the continuity equation to recover the ellipticity, while retaining the iterative SIMPLE Poisson pressure correction equation approach. In practise this leads to a similar discretization to the Rhies and Chow scheme [5], which uses interpolation of the momentum equations to mimic the SIMPLE scheme, but on a non-staggered mesh, with identical ellipticity. Such schemes were defined to be strongly elliptic, and it was suggested that strong ellipticity was a desirable feature of any scheme and this was one of the reasons for the popularity of the SIMPLE scheme. A discrete ellipticity measure E_h, defined in Section 3, was proposed by Armfield such that the SIMPLE scheme had $E_h = 1$ and non-elliptic schemes had $E_h = 0$. A strongly elliptic scheme was then defined to be one with $E_h > 0.66$.

As noted above, in the Armfield scheme and in many other schemes [2, 3], the full ellipticity of the continuous equations is recovered by adding additional terms into the continuity equation. The terms introduced by Armfield, referred to as the elliptic correction terms in the remainder of this paper, are presented in the next section. Typically these terms are dependent on the grid size and as a result introduce an additional truncation error into the scheme. As this additional error may affect the overall accuracy, it has been suggested in the context of another method that their magnitude should be reduced by multiplying them by a factor of 0.1 [3]. If this approach is taken the degree of ellipticity of the discrete equations will be reduced, resulting in a weakly elliptic system. It was suggested by Armfield that weakly elliptic schemes may not be able to prevent the occurrence of the grid scale pressure oscillation; however, subsequent investigation has shown that only a small degree of ellipticity is required to prevent this phenomenon for the flows considered. In this paper the effect of including such a multiplying factor with the elliptic correction terms proposed by Armfield is considered. It is shown that, although strong ellipticity is not necessary to prevent the grid-scale pressure oscillation, the degree of ellipticity has an influence on the rate of convergence. Thus the use of a multiplying factor to reduce the magnitude of the elliptic correction terms, to in turn reduce the associated error, will also reduce the rate of convergence.

A detailed analysis of the error associated with the inclusion of the elliptic correction terms has been carried out and

0021-9991/94 $6.00

it is shown that this error is a combination of the additional truncation error in the continuity equation together with, in finite volume schemes using the conservation form of the governing equations, a false source arising from the discretization of the advection terms. The additional truncation error is of the same order as the truncation error of the unmodified continuity equation. The false source error, although also relatively small, may be removed entirely by using a consistent method for the construction of the conservation form of the governing equations. It is shown that the inclusion of the full elliptic correction terms does not have a significant influence on the solution for the flow considered, and thus the convergence advantages of the strongly elliptic scheme may be retained.

The remainder of the paper is as follows. In Section 2 the numerical method, including the form of the elliptic correction terms, is briefly described. In Section 3 a definition of the discrete ellipticity measure E_h is given, the method of varying the ellipticity of the scheme is described, an estimate is obtained for the order of the correction terms, and the consistent derivation of the conservation form of the governing equations is presented. In Section 4 a comparison of the solutions obtained with varying ellipticities is presented, together with truncation error and convergence results. Section 5 contains the discussion and conclusions.

2. METHOD

For simplicity only the momentum and continuity equations are presented in the description of the numerical method. Results in Section 4 are presented for natural convection flow and this requires the inclusion of a temperature equation. Its conclusion is accomplished in exactly the same manner as for any SIMPLE-type scheme and does not affect the pressure–velocity coupling and the elliptic correction terms, which are the primary subject of this paper. For the results presented in Secion 4 the Boussinesq assumption is made for buoyancy, allowing for the incompressible Navier–Stokes equations to be used.

2.1. *Governing Equations*

The Navier–Stokes equations are expressed in non-dimensional form in cartesian coordinates (x, y) with corresponding velocity components (U, V) and P the pressure as follows,

$$U_t + UU_x + VU_y = -P_x + \frac{1}{\mathrm{Re}}(U_{xx} + U_{yy}) \tag{1}$$

$$V_t + UV_x + VV_y = -P_y + \frac{1}{\mathrm{Re}}(V_{xx} + V_{yy}) \tag{2}$$

$$U_x + V_y = 0, \tag{3}$$

where subscripts indicate partial differentiation, the Reynolds number $\mathrm{Re} = \bar{U}L/\nu$, with $\bar{U}$ being a characteristic velocity and L a characteristic length.

2.2. *Discretisation*

The equations are discretised on a rectangular mesh, with x^i denoting the ith node in the x direction and y^j denoting the jth node in the y direction. Finite volumes are used to convert differential terms in the governing equations in the following way. All second derivatives are approximated by second-order central differences as

$$U_{xx}(x^i, y^j) = \left(\frac{U^{i+1} - U^i}{\Delta x^{i+1}} - \frac{U^i - U^{i-1}}{\Delta x^i}\right)^j \Big/ \left(\frac{\Delta x^{i+1} + \Delta x^i}{2}\right) + O(\Delta x^2) = SDU^{ij}, \tag{4}$$

where $\Delta x^i = x^i - x^{i-1}$ and SD is a finite difference operator.

Derivatives occurring in convective terms, which are written in conservation form, are approximated using a third-order QUICK scheme [11], as

$$(UU)_x(x^i, y^j) = (F^{i+1/2,j} - F^{i-1/2,j})\, 2/(\Delta x^{i+1} + \Delta x^i) + O(\Delta x^3), \tag{5}$$

where

$$F^{i+1/2,j} = [U^{i+1/2}(U^{i+1/2} - SDU^i(\Delta x^{i+1})^2/8)]^j,$$
$$F^{i-1/2,j} = [U^{i-1/2}(U^{i-1/2} - SDU^{i-1}(\Delta x^i)^2/8)]^j,$$

assuming that $U^{i+1/2,j}$ and $U^{i-1/2,j}$ are positive. Discrete forms for the pressure and divergence terms are given below.

2.3. *Time Integration*

The above equations are integrated numerically in the following way. All variables are known at time step t^n. First an initial estimate for $(U, V)^{n+1}$ is obtained, denoted as $(U, V)^{n+1,m}$ with $m = 0$, from

$$G1(U^{n+1,m}) = G2(U^n) - (P^{i+1} - P^{i-1})^{j,n+1/2,m}/(\Delta x^{i+1} + \Delta x^i),$$
$$G1(V^{n+1,m}) = G2(V^n) - (P^{j+1} - P^{j-1})^{i,n+1/2,m}/(\Delta y^{j+1} + \Delta y^j).$$

$G1 = (L/2 + 1/\Delta t)$, $G2 = (-L/2 + 1/\Delta t)$, and L is in discrete form a block quinta-diagonal matrix, with components obtained from the discretisation described above, which may be inverted using any of the standard techniques. The best available guess is used for $P^{n+1/2,0}$. Next a correction

for P is obtained by solving the following Poisson equation for Pc, the pressure correction,

$$\left[g^{i+1/2}\left(\frac{Pc^{i+1}-Pc^{i}}{\Delta x^{i+1}}\right)-g^{i-1/2}\left(\frac{Pc^{i}-Pc^{i-1}}{\Delta x^{i}}\right)\right]^{j}\times 2/(\Delta x^{i+1}+\Delta x^{i})+\left[g^{j+1/2}\left(\frac{Pc^{j+1}-Pc^{j}}{\Delta y^{j+1}}\right)-g^{j-1/2}\left(\frac{Pc^{j}-Pc^{j-1}}{\Delta y^{j}}\right)\right]^{i}\times 2/(\Delta y^{j+1}+\Delta y^{j})=(\bar{U}^{i+1/2}-\bar{U}^{i-1/2})^{j,n+1,m}\,2/(\Delta x^{i+1}+\Delta x^{i})+(\bar{V}^{j+1/2}-\bar{V}^{j-1/2})^{i,n+1,m}\,2/(\Delta y^{j+1}+\Delta y^{j}),\qquad(6)$$

where g is the inverse of the diagonal of $G1$. As can be seen this is a finite volume discretisation about the point (i,j) consisting of, in the x direction for example, the difference of the terms $g(Pc)_x$ and $\bar{U}$ at the points $x=x^{i+1/2}$, $x=x^{i-1/2}$, and similarly for the y terms.

The $P^{n+1/2,m}$, $U^{n+1,m}$, and $V^{n+1,m}$ are then corrected as

$$U^{i,j,n+1,m+1}=U^{i,j,n+1,m}-[g^{i}(Pc^{i+1}-Pc^{i-1})]^{j}/(\Delta x^{i+1}+\Delta x^{i}),$$

$$V^{i,j,n+1,m+1}=V^{i,j,n+1,m}-[g^{j}(Pc^{j+1}-Pc^{j-1})]^{i}/(\Delta y^{j+1}+\Delta y^{j}),$$

and

$$P^{i,j,n+1/2,m+1}=RxPc^{i,j}+P^{i,j,n+1/2,m},$$

with Rx an under-relaxation factor for the pressure, which for the present simulation was set to 0.6. The iteration index is then set to $m=m+1$ and the process is repeated until a divergence-free velocity field that satisfies the momentum equations is obtained.

The terms $\bar{U}$ and $\bar{V}$ are interpolated velocities defines as

$$\bar{U}^{i+1/2,j}=(U^{i+1}+U^{i})^{j}/2+R^{i+1/2,j},$$

$$\bar{V}^{j+1/2,i}=(V^{j+1}+V^{j})^{i}/2+R^{j+1/2,i},$$

with the R terms defined as

$$R^{i+1/2,j}=\left[\left\{g^{i+1}\left(\frac{P^{i+2}-P^{i}}{\Delta x^{i+2}+\Delta x^{i+1}}\right)+g^{i}\left(\frac{P^{i+1}-P^{i-1}}{\Delta x^{i+1}+\Delta x^{i}}\right)\right\}\Big/2-g^{i+1/2}\left(\frac{P^{i+1}-P^{i}}{\Delta x^{i+1}}\right)\right]^{j},\qquad(7)$$

$$R^{j+1/2,i}=\left[\left\{g^{j+1}\left(\frac{P^{j+2}-P^{j}}{\Delta y^{j+2}+\Delta y^{j+1}}\right)+g^{j}\left(\frac{P^{j+1}-P^{j-1}}{\Delta y^{j+1}+\Delta y^{j}}\right)\right\}\Big/2-g^{j+1/2}\left(\frac{P^{j+1}-P^{j}}{\Delta y^{j+1}}\right)\right]^{i}.\qquad(8)$$

The R terms as defined above are the elliptic correction terms that ensure that the discretisation is strongly elliptic with ellipticity measure, as defined below, of $E_h=1$. As a result of the inclusion of these terms the pressure velocity coupling is identical to that of a compact second-order differencing of the Laplace operator, whereas otherwise the coupling is equivalent to a sparse $2h$ differencing and is non-elliptic, with $h=\Delta x=\Delta y$ for convenience in notation, although in general it is not necessary that $\Delta x=\Delta y$. The R terms will combine in the Poisson pressure correction equation to form the difference between a sparse and a compact discretisation of the Laplacian of P. These operators could be included directly into the continuity equation, as noted below; however, expressing them in the form shown here simplifies the inclusion of boundary conditions for finite volume schemes, in which boundary conditions are applied by including an additional point outside the domain. The gradient of the pressure correction is set to zero at the boundary, while the pressure at the exterior point is obtained by a second-order extrapolation from the interior.

3. ANALYSIS

The discrete *h-ellipticity* measure, E_h, of a discrete operator L, is defined as [1]

$$E_h=\rho\pi\leqslant\operatorname*{Min}_{|\boldsymbol{\theta}|,\,|\boldsymbol{\theta}'|\leqslant\pi}\frac{\hat{C}(\boldsymbol{\theta}')}{\hat{C}(\boldsymbol{\theta})}\left|\frac{\hat{L}(\boldsymbol{\theta})}{\hat{L}(\boldsymbol{\theta}')}\right|,\qquad(9)$$

where $\boldsymbol{\theta}$ is the wave number, $\hat{L}$ is the symbol of L, $0<\rho<1$, and $\hat{C}$ is the symbol of the compact five-point Laplace operator, ∇_b^2 below. This measure, which is a variation of the measure suggested by Brandt and Dinar [12], normalises the difference in amplitude of $\hat{L}$ at different wave numbers by that of the standard five-point compact Laplacian, which then has an E_h of 1, and for good ellipticity it is required that E_h not be small, compared to 1. A non-elliptic operator will have $E_h=0$.

The method considered in the present paper may best be analysed by writing the steady-state Navier–Stokes equations in operator form as

$$L(u)+Dpx(p)=0,$$

$$L(v)+Dpy(p)=0,$$

$$Dvx(u)+Dvy(v)+L^{-1}(\nabla_a^2(p)-\nabla_b^2(p))=0.$$

The above system has been written in a form in which the pressure gradients and divergence operators appear explicitly as the D operators. It is convenient to use different notations for these operators to allow a clearer exposition of the analysis. The ∇_a^2 and ∇_b^2 terms included in the continuity equation represent the elliptic correction terms given in Eqs. (7) and (8) in Section 2 above. It is clear that the above system in the continuous form is identical to the governing equations; however, if different discretisations are used for the $._a$ and $._b$ Laplace operators then the system will not be identical in discrete form [1].

All D terms are discretised using central differences, while a sparse $2h$ differencing is used for ∇_a^2 and a compact h differencing, for ∇_b^2. That is,

$$\nabla_a^2(p) = (2h)^{-2}((p^{i+2}+p^{i-2})^j + (p^{j+2}+p^{j-2})^i - 4p^{i,j}),$$
$$\nabla_b^2(p) = h^{-2}((p^{i+1}+p^{i-1})^j + (p^{j+1}+p^{j-1})^i - 4p^{i,j}).$$

When the form of the Navier–Stokes equations given above is transformed into wave number space it is represented by the following matrix system,

$$\begin{bmatrix} \hat{L} & 0 & \widehat{Dpx} \\ 0 & \hat{L} & \widehat{Dpy} \\ \widehat{Dvx} & \widehat{Dvy} & \hat{L}^{-1}(\hat{\nabla}_a^2(p) - \hat{\nabla}_b^2(p)) \end{bmatrix} \begin{matrix} \hat{u} \\ \hat{v} = 0, \\ \hat{p} \end{matrix} \quad (10)$$

where $\hat{}$ represents the Fourier transform of the discrete operator and a linearised form of the non-linear operator L is being considered. The symbol of the numerical method is then the determinant of the symbolic matrix given above, and ellipticity requires that the symbol is non-zero for all realisable high wave-number components. The determinant of the symbolic matrix is

$$\text{Det} = \hat{L}(\hat{\nabla}_a^2 - \hat{\nabla}_b^2 - \widehat{Dvy}\,\widehat{Dpy} - \widehat{Dvx}\,\widehat{Dpx}).$$

By retaining the Dvy, Dpy, Dvx, Dpx operators, which combine to give $\widehat{Dvy}\,\widehat{Dpy} + \widehat{Dvx}\,\widehat{Dpx} = \hat{\nabla}_a^2$, it is possible to see that the pressure/continuity interaction results in a Laplace operator and that

$$\text{Det} = -\hat{L}\hat{\nabla}_b^2.$$

Assuming that L is differenced in such a way so as not to effect the ellipticity of the system, the ellipticity of this scheme is determined by the pressure–continuity coupling which has the symbol ∇_b^2. As a compact h discretisation has been chosen for ∇_b^2 the ellipticity of this system is identical to that of a compact h discretisation of the Laplace operator and is, therefore, strongly elliptic with $E_h = 1$. It should be noted that in the method described in Section 2 the inverse of L is not actually used. Rather, the standard SIMPLE approximation to the inverse is used, that is, the inverse of the matrix of diagonal terms. As with the SIMPLE scheme itself the use of an iterative approach with this approximation results in the fully inverted matrix being obtained implicitly.

The method presented above is easily modified to change the degree of ellipticity by including a multiplying factor M with the additional terms in the continuity equation as

$$\begin{aligned} L(u) + Dpx(p) &= 0, \\ L(v) + Dpy(p) &= 0, \quad (11) \\ Dvx(u) + Dvy(v) + ML^{-1}(\nabla_a^2(p) - \nabla_b^2(p)) &= 0. \end{aligned}$$

The determinant of the matrix of the system including the multiplier is then

$$\text{Det} = \hat{L}(M(\hat{\nabla}_a^2 - \hat{\nabla}_b^2) - \widehat{Dvy}\,\widehat{Dpy} - \widehat{Dvx}\,\widehat{Dpx}),$$

which may be written as

$$\text{Det} = -\hat{L}(M\hat{\nabla}_b^2 + (1-M)\,\hat{\nabla}_a^2).$$

The discrete ellipticity measure of the modified scheme, as defined in Armfield [1], is then $E_h = 2M/(M+1)$. In practise the inclusion of the multiplying factor is accomplished by multiplying the R terms in Eqs. (7) and (8) above by M.

3.1. *Truncation Error*

The inclusion of the elliptic correction terms will add an additional truncation error to the discrete continuity equation, reducing the degree to which it approximates the continuous equation. This additional error may be analysed in the following way. When the terms ∇_a^2 and ∇_b^2 are expanded and combined we obtain in the x direction

$$\frac{P^{i+2} - 2P^i + P^{i-2}}{4\Delta x^2} - \frac{P^{i+1} - 2P^i + P^{i-1}}{\Delta x^2} = \frac{\Delta x^2}{4}\left[\frac{P^{i+2} - 4P^{i+1} + 6P^i - 4P^{i-1} + P^{i-2}}{\Delta x^4}\right],$$

which is a second-order discretisation for $\Delta x^2 P_{xxxx}$, and similarly for the y direction. The correction is then seen to be equal to L^{-1} multiplied by a central finite volume discretisation of the fourth-order derivatives of pressure,

$$P_{\text{cor}} = L^{-1}\left[\frac{(\Delta x)^2}{4} P_{xxxx} + \frac{(\Delta y)^2}{4} P_{yyyy}\right]. \quad (12)$$

As the magnitude of the term L^{-1} in discrete form will be dominated by the time difference term $1/\Delta t$ for small enough Δt, the overall order of the additional truncation error

associated with the elliptic correction terms is expected in the limit to behave as $h^2\,\Delta t$. The leading order truncation term in the second-order finite volume discretisation of the unmodified continuity equation is of order h^2 and, therefore, it is expected that the additional error associated with the elliptic correction terms will not significantly increase the truncation error of the discrete continuity equation. This is examined in detail in Section 4.

3.2. *Conservation Error*

In finite volume schemes of the type used here the momentum equations and any additional transport equations are converted to a conservation form before being discretised. Thus, for instance, the U momentum equation,

$$U_t + UU_x + VU_y = -P_x + \frac{1}{\mathrm{Re}}(U_{xx} + U_{yy}),$$

is converted to

$$U_t + (UU)_x + (VU)_y = -P_x + \frac{1}{\mathrm{Re}}(U_{xx} + U_{yy}),$$

by expressing the advection term as

$$UU_x + VU_y + U(U_x + V_y),$$

to obtain

$$(UU)_x + (VU)_y,$$

the conservation form of the U-momentum advection terms. Although in continuous form the divergence $U_x + V_y = 0$, allowing the above construction, in discrete form this constraint is not exactly satisfied, and thus a false source of the form $U\,\mathrm{Div}(U, V)$ is included in the equation. As the residual of the divergence is the commonly specified convergence criterion for schemes of this type, $\mathrm{Div}(U, V)$ is small, and thus the effect of the false source is also small. However, when the elliptic correction terms are included in the continuity equation it is the residual of the modified equation that is driven to the convergence criterion [3], and as a result an additional false source is implicitly included in the momentum equation of the form, $-UP_{\mathrm{cor}}$. This effect may be significant particularly in problems with very long integration times.

The false source term described above may be removed by constructing the conservation equations in a consistent manner, which may be accomplished in two ways. The $(\bar{U}, \bar{V})$ velocities may be stored and used directly in the advection terms; then as $\mathrm{Div}(\bar{U}, \bar{V})$ is driven to convergence the false source term will be small. Such an approach is similar to that used by Rhies and Chow [5]. An alternative method is used here whereby the conservation equations are constructed using the modified continuity equation including the elliptic correction terms. When this is done an additional source term of the form UP_{cor} is obtained that must be included explicitly into the u-momentum equation, and similarly for the other transport equations that are being solved, cancelling out the implicit false source given above. In practise to obtain P_{cor} it is not necessary to evaluate the fourth derivatives of pressure; rather the difference between the modified and unmodified divergence is used. The influence of this term on the solution is considered in detail in the next section.

4. RESULTS

Results have been obtained for the transient behaviour of natural convection flow in a square cavity subjected impulsively to a horizontal temperature gradient at a Rayleigh number of 6×10^8. The Rayleigh number is defined as $\mathrm{Ra} = g\beta H^3(\Delta T)/\nu\kappa$, with g the acceleration due to gravity, β the coefficient of thermal expansion, H the height of the cavity, ΔT the total temperature variation in the cavity, ν the kinematic viscosity, and κ the thermal diffusivity.

The top and bottom of the cavity are insulated and the side walls are set to $\pm\Delta T/2$, with all boundaries non-slip. The fluid, which is assumed to be water with Prandtl number $\mathrm{Pr} = 7.5$ and kinematic viscosity $\nu = 1 \times 10^{-6}\,\mathrm{m^2 s^{-1}}$, is initially at rest and isothermal, the heating and cooling is then switched on instantaneously and the flow is traced as it evolves to steady state. A full description of the flow is given in Patterson and Armfield [13] and Armfield and Patterson [14] and the reader is referred to those papers for details which will not be given here. The results presented below were obtained with a convergence criterion at each

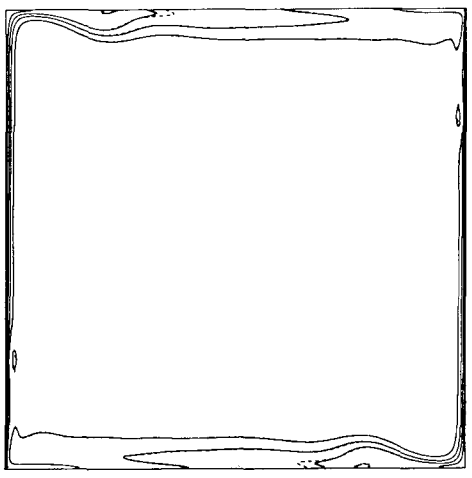

FIG. 1. Temperature contours for $M = 1.0$ (dashed line), $M = 0.1$ (dotted line), and $M = 0.0$ (solid line).

time step of the integrated absolute residual of the modified continuity equation being less than 1×10^{-4}. The code was run on a STAR 910VP [15].

The temperature contours obtained with M values of 1.0, 0.1, and 0.0, after 500 time steps, are presented in Fig. 1. These results were obtained on a non-uniform 99×99 mesh with grid stretching used to place additional points in regions of high variation adjacent to the boundaries. The non-dimensional time step is $\Delta t = 0.002$ (0.29s), based on the cavity height of $H = 0.24$m and a charactersitic velocity $\bar{U} = 1.67 \times 10^{-3}\text{ms}^{-1}$. The solution at 500 time steps has been chosen for the presentation of results as it allows a comparison between the non-zero M and the $M = 0.0$ solutions. When the integration is continued past the 500th time step for $M = 0.0$ the solution ceases to converge at approximately 700 time steps due to the grid scale pressure oscillation discussed above.

The hot wall is on the left and thermal intrusions travelling across the ceiling and floor are clearly visible. A variation with respect to M can be seen in the cold intrusion approximately one-third of the way across the cavity from the cold wall and at a corresponding location in the hot intrusion. The variation is more easily seen in Fig. 2a, which contains an expansion of the cold intrusion. This clearly shows that the variation is greatest between the $M = 1.0$ and the other two results, the $M = 0.1$ and $M = 0.0$ solutions, which are almost identical. It should be noted that this variation occurs in a region of relatively small gradient, and as contours are shown the variation corresponds to only a small absolute difference in the temperature. Apparently the temperature field has developed more rapidly for the $M = 1.0$ solution than the for the $M = 0.1$ and the $M = 0.0$ results.

Figure 2b contains an expansion of the same region for the $M = 1.0$ and $M = 0.0$ solutions, but with the $M = 1.0$ solution now obtained using the consistently derived conservation form of the advection terms, as described in Section 3.2 above, thus removing the false source associated with the inconsistent derivation. The consistent derivation of the advection terms has had an effect on the discrepancy noted above, effectively removing most of the variation associated with the $M = 1.0$ result, and the two solutions are now in close agreement.

Contours of the U and V velocity fields and the pressure P show no discernible variation with M; for brevity these results are not presented.

To enable a more quantitative comparison of the solutions obtained for the different M values the normalised integral of the absolute difference of the $M = 1.0$, $M = 0.1$, and the consistently derived $M = 1.0$ solutions with respect to the $M = 0.0$ solution are presented in Table I. For instance, the error for the $M = 1.0$ pressure result is defined as

$$\frac{\int_D |P_{M=1} - P_{M=0}|}{\int_D |P_{M=0}|}.$$

All of the fields have an error $\sim 2\%$ for the $M = 1.0$ solution, although as noted above only the temperature contours showed a discernible variation due to the low gradients of temperature in the intrusions. When the consistent $M = 1.0$ solution is considered it is seen that the error is reduced by approximately 65% for the pressure, the velocities and the temperature, compared to the standard $M = 1.0$ solution. Apparently this reduction is sufficient to remove most of the observed error in the temperature contours, as noted in Fig. 2b above. For the $M = 0.1$ solution the error is reduced by approximately 90%, as is expected.

Figure 3 contains results comparing the integral of the leading order truncation term for the second-order unmodified continuity equation with the integral of the elliptic correction terms, for a range of grid sizes. Thus the integral of the leading order truncation term is

$$\int_D \left| \frac{\Delta x^2}{6} U_{xxx} \right| + \left| \frac{\Delta y^2}{6} V_{yyy} \right|, \tag{13}$$

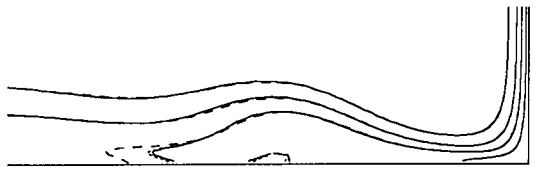

FIG. 2. (a) Expanded temperature contours in the cold intrusion for $M = 1.0$ (dashed line), $M = 0.1$ (dotted line), and $M = 0.0$ (solid line).

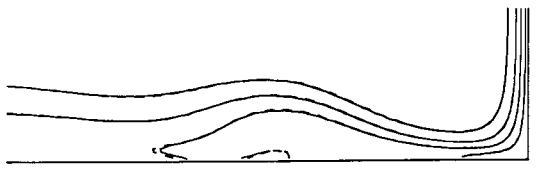

FIG. 2. (b) Expanded temperature contours in cold intrusion for $M = 1.0$ with the consistent derivation (solid line) and $M = 0.0$ (dashed line).

TABLE I

Integral of the Variation of the $M = 1.0$, $M = 0.1$, and Consistent $M = 1.0$ Solutions with Respect to the $M = 0.0$ Solution

Field	$M = 1.0$	$M = 0.1$	$M = 1.0$ (consistent)
Pressure	0.012	0.0012	0.0039
u-velocity	0.019	0.0020	0.0080
v-velocity	0.018	0.0019	0.0072
Temperature	0.022	0.0022	0.0085

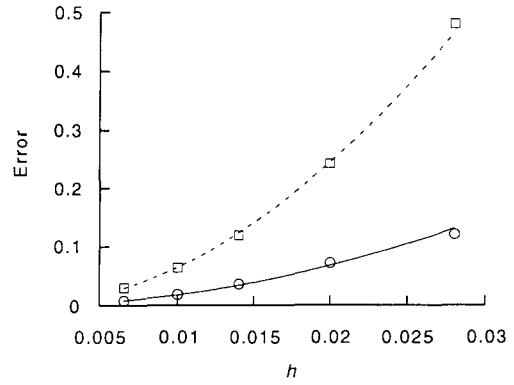

FIG. 3. Error plotted against grid size for the integral of the leading order truncation term of the unmodified continuity equation (□) and the integral of the elliptic correction terms (○) with least squares power law fit.

while the integral of the elliptic correction terms is obtained as

$$\int_D |\mathrm{Div}(U, V) - \mathrm{Div}(\bar{U}, \bar{V})|, \tag{14}$$

where $\mathrm{Div}(U, V)$ is the discrete divergence obtained by a second-order finite volume differencing and $\mathrm{Div}(\bar{U}, \bar{V})$ is the discrete divergence of the corrected velocities as given in Section 2.3 above. A least squares fit was used to determine the power dependence of the error in the form error $= h^r$. For the unmodified continuity truncation term $r = 1.93$ was obtained, while for the correction term $r = 1.92$ was obtained. Clearly both sets of results are exhibiting a quadratic behaviour with respect to the grid size, and it is observed that the magnitude of the unmodified truncation error is typically four times that of the elliptic correction terms over the range of grid sizes presented. It should be noted that for this flow a non-uniform grid is used and the grid-size for the comparison made above is an averaged value. The five grid sizes calculated correspond to 35×35, 49×49, 71×71, 99×99, and 150×150 grids all obtained with a time-step of $\Delta t = 0.002$.

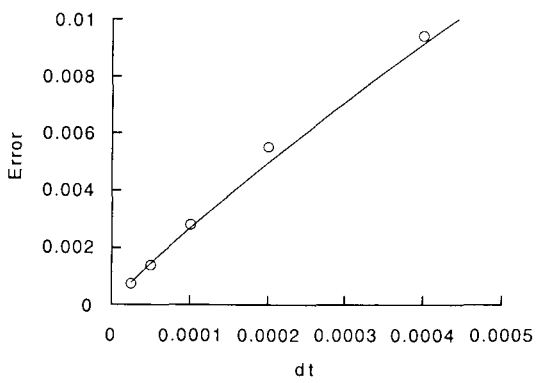

FIG. 4. Integral of the elliptic correction terms plotted against time-step with least squares power law fit.

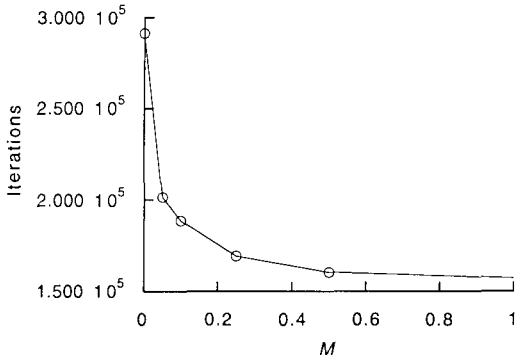

FIG. 5. Total iteration count plotted against M.

The behaviour of the error associated with the elliptic correction terms with respect to the time-step is shown in Fig. 4, where the integral of the elliptic correction terms, as defined above, is plotted against the time-step for a range of time-steps, all on the 99×99 grid. Once again a least squares fit was used to determine the power dependence of the error in the form error $= \Delta^r$ with $r = 0.898$ being obtained. The elliptic correction error therefore displays an approximately linear variation with respect to the time step.

Figure 5 contains iteration counts for a range of multiplying factors and, hence, ellipticities of $0.0 \leqslant M \leqslant 1.0$. The iteration count presented represents the total number of sweeps of the Poisson solver used to solve the temperature equation, the momentum equation and the pressure correction equation for 500 time steps from initialisation on the 99×99 grid with time step $\Delta t = 0.002$. As can be seen the number of iterations increases with decreasing ellipticity, with the $M = 0.0$ case requiring approximately twice the iterations of the $M = 1.0$ case. As noted above when the code is continued past the 500th time step the $M = 0.0$ case will cease to converge at approximately 700 time steps, as a result of the grid-scale oscillation in the pressure field. For all non-zero M values tested the code continues to run to steady state, which is reached after approximately 5000 time steps, with the variation in iteration count being approximately the same as that shown in Fig. 5.

5. DISCUSSION AND CONCLUSIONS

It has been shown both analytically and experimentally that the additional error introduced by the inclusion of the elliptic correction terms proposed by Armfield [1] into the continuity equation is second order in space and first order in time, and thus the modified equations are still a consistent approximation of the continuous equations. Nonetheless if the error associated with the elliptic correction terms is significant the need to reduce the grid size and/or time

step significantly below that which would otherwise be used will lead to an inefficient scheme. An alternative to reducing the grid size is to reduce the magnitude of the elliptic correction terms by including a multiplying factor set to less than 1.0, as suggested by Sotiropoulos and Abdallah [10] who recommended $M = 0.1$. Although this will have the effect of reducing the error by an order of magnitude it will also reduce the degree of ellipticity of the scheme.

The error associated with the introduction of the elliptic correction terms into the continuity equation consists of two components when a conservative finite volume scheme is used. One component is a direct result of the increase in the truncation error of the continuity equation, while the other is associated with the derivation of the conservation equations. When the conservation equation are constructed it is assumed that the divergence of the velocity will be zero. While this is never true in a numerical method, the discrete divergence is generally close to machine zero, as it is the commonly specified convergence criterion for schemes of this type. However, when the elliptic correction terms are included, although the modified discrete divergence will be close to machine zero, the unmodified discrete divergence will be considerably larger. This error is thus a result of the modified continuity equation being driven to convergence, while the unmodified continuity equation is used to construct the conservation equations. The conservation error is grid dependent and a further refinement of the grid will reduce its magnitude; however, it is easily removed entirely by constructing the conservation equations in a consistent manner, using the modified continuity equation, or by storing and using the $(\bar{U}, \bar{V})$ velocities directly in the advection terms.

The error associated with the change in the truncation error of the continuity equation, cannot be removed from the scheme entirely, although it may be reduced in magnitude by including a multiplying factor as suggested by Sotiropoulos and Abdallah [3]. However as the leading order truncation term in the unmodified continuity equation and the elliptic correction terms are both second order and, at least for the flow considered, the unmodified truncation term is larger than the elliptic correction terms, it is likely that the direct influence on the solution of the elliptic correction terms will be small. This has been demonstrated by showing that the $M = 1.0$ solution has only $\sim 2\%$ variation when compared to the $M = 0.0$ solution. It should also be noted that the flow considered here is a relatively severe test of the effect of the inclusion of the elliptic correction terms, due to the considerable pressure gradients that are associated with the stratified intrusions.

The magnitude of the elliptic correction terms is therefore a good measure of the overall accuracy of the scheme for the flow considered. If they are large then it is likely that the leading order truncation term of the unmodified continuity equation is also large and that a finer grid is required to obtain an accurate solution, with or without the inclusion of the correction terms. Although the error associated with the correction terms can be separately reduced by reducing M, it is suggested that this approach should only be taken when it has been ascertained that the unmodified equations do not require a further grid refinement.

In addition to the effect of the error resulting from the introduction of the elliptic correction terms, this paper has also considered the effect of the degree of ellipticity on the rate of convergence of the scheme. From the results presented in the previous section it is clear that the degree of ellipticity of the discrete Navier–Stokes equations has a significant influence on the rate of convergence, with a reduction in ellipticity from $E_h = 1.0$ to $E_h = 0.18$ $(M = 0.1)$ resulting in an increase of 20% in the iteration count and consequently in computer time. In the method presented the reduction in ellipticity is associated with a reduction in the degree of the grid-scale smoothing, and thus the reduction in the rate of convergence is associated with the increased number of iterations required to smooth the grid-scale error. The reason that the rate of convergence does not have a one-to-one relationship with the grid-scale ellipticity is [presumably] because schemes of the type considered are proportionally more efficient at smoothing the high wave number error. If this were not the case then a reduction of a factor of two in ellipticity would result in an increase of a factor of two in cpu time. Multi-grid schemes, in which a proportionally smaller amount of time is spent on smoothing the grid-scale error, may result in a greater influence of the degree of ellipticity of the grid scale on the rate of convergence.

It is also observed that, even when the magnitude of the elliptic terms is reduced by a factor of 10, no oscillation is seen in the pressure field. In fact, of the M values tested, only the $M = 0.0$, the non-elliptic case, showed an oscillation in the pressure, which after a sufficient number of time steps prevented convergence. It is therefore clear for this flow that even relatively weakly elliptic schemes will still retain enough ellipticity to prevent the pressure oscillation, in contradiction to the suggestion of Armfield [1]. However, the use of strongly elliptic schemes may still be recommended on the basis of more rapid convergence, while if a conservative finite volume scheme is used the conservation equations should be constructed in a consistent fashion using the modified continuity equation, including the elliptic correction terms.

REFERENCES

1. S. Armfield, *Comput. Fluids* **20**, 1 (1991).
2. J. C. Strikewerda, *SIAM J. Sci. Stat. Comput.* **5**, 56 (1984).
3. S. Abdallah, *J. Comput. Phys.* **70**, 182 (1987).
4. G. Schneider and M. Raw, *Numer. Heat Transfer* **11**, 363 (1987).
5. C. M. Rhies and W. L. Chow, AIAA-82-0988, 1982 (unpublished).

6. V. Pratap and D. Spalding, *Int. J. Heat Mass Transfer* **19**, 1183 (1976).
7. S. Patankar, *Numerical Heat Transfer and Fluid Flow* (Hemisphere, McGraw–Hill, New York, 1980).
8. L. Caretto, A. Gosman, S. Patankar, and D. Spalding, in *Proceedings, Third International Conference on Numerical Methods in Fluid Dynamics* (Springer Verlag, New York, 1972).
9. S. Connell and P. Stow, *Comput. & Fluids* **14**, 1 (1986).
10. F. Sotiropoulos and S. Abdallah, *J. Comput. Phys.* **95**, 212 (1991).
11. B. P. Leonard, *Comput. Methods Appl. Mech. Eng.* **19**, 59 (1979).
12. A. Brandt and N. Dinar, in *Proceedings, Conference on Numerical solutions of Partial Differential Equations, Mathematical Research Centre, Madison, WI, October 1978.*
13. J. C. Patterson and S. W. Armfield, *J. Fluid Mech.* **219**, 469 (1990).
14. S. Armfield and J. C. Patterson, *Int. J. Heat Mass Transfer* **34**, 929 (1991).
15. S. Armfield, *Int. J. Numer. Methods Fluids* **17**, 589 (1993).